

Measurement of double beta decay of ^{100}Mo to excited states in the NEMO 3 experiment

R. Arnold ^{a,*}, C. Augier ^b, J. Baker ^c, A.S. Barabash ^d,
M. Bongrand ^b, G. Broudin ^e, V. Brudanin ^f, A.J. Caffrey ^c,
V. Egorov ^f, A.I. Etienvre ^b, N. Fatemi-Ghomi ^g, F. Hubert ^e,
Ph. Hubert ^e, J. Jerie ^h, C. Jollet ^a, S. Jullian ^b, S. King ⁱ,
O. Kochetov ^f, S.I. Konovalov ^d, V. Kovalenko ^f, D. Lalanne ^b,
T. Lamhamdi ^j, F. Leccia ^e, Y. Lemièrè ^k, C. Longuemare ^k,
G. Lutter ^e, Ch. Marquet ^e, F. Mauger ^k, A. Nachab ^e,
H. Ohsumi ^l, F. Perrot ^e, F. Piquemal ^e, J.L. Reyss ^m,
J.S. Ricol ^e, R. Saakyan ⁱ, X. Sarazin ^b, L. Simard ^b,
F. Šimkovic ⁿ, Yu. Shitov ^f, A. Smolnikov ^f,
S. Söldner-Rembold ^g, I. Štekl ^h, J. Suhonen ^o, C.S. Sutton ^p,
G. Szklarz ^b, J. Thomas ⁱ, V. Timkin ^f, V. Tretyak ^f,
V. Umatov ^d, L. Vála ^h, I. Vanyushin ^d, V. Vasiliev ⁱ,
V. Vorobel ^q, Ts. Vylov ^f

NEMO Collaboration

^a*IPHC, IN2P3-CNRS et Université Louis Pasteur, F-67037 Strasbourg, France*

^b*LAL, IN2P3-CNRS et Université Paris-Sud, F-91405 Orsay, France*

^c*INEEL, Idaho Falls, ID83415, USA*

^d*Institute of Theoretical and Experimental Physics, 117259 Moscow, Russia*

^e*CENBG, IN2P3-CNRS et Université Bordeaux I, F-33170 Gradignan, France*

^f*Joint Institute for Nuclear Research, 141980 Dubna, Russia*

^g*University of Manchester, M13 9PL Manchester, United Kingdom*

^h*IEAP, Czech Technical University in Prague, CZ-12800 Prague, Czech Republic*

ⁱ*University College London, WC1E 6BT London, United Kingdom*

^j*USMBA, Fes, Maroc*

^k*LPC, IN2P3-CNRS et Université de Caen, F-14032 Caen, France*

^l*Saga University, Saga 840-8502, Japan*

^m*LSCE, CNRS, F-91190 Gif-sur-Yvette, France*

ⁿ*FMFI, Comenius University, SK-842 48 Bratislava, Slovakia*

^o*Jyväskylä University, 40351 Jyväskylä, Finland*

^p*MHC, South Hadley, Massachusetts, MA01075, USA*

^q*Charles University, Prague, Czech Republic*

Abstract

The double beta decay of ^{100}Mo to the 0_1^+ and 2_1^+ excited states of ^{100}Ru is studied using the NEMO 3 data. After the analysis of 8024 h of data the half-life for the two-neutrino double beta decay of ^{100}Mo to the excited 0_1^+ state is measured to be $T_{1/2}^{(2\nu)} = [5.7_{-0.9}^{+1.3}(\text{stat}) \pm 0.8(\text{syst})] \cdot 10^{20}$ y. The signal-to-background ratio is equal to 3. Information about energy and angular distributions of emitted electrons is also obtained. No evidence for neutrinoless double beta decay to the excited 0_1^+ state has been found. The corresponding half-life limit is $T_{1/2}^{(0\nu)}(0^+ \rightarrow 0_1^+) > 8.9 \cdot 10^{22}$ y (at 90% C.L.).

The search for the double beta decay to the 2_1^+ excited state has allowed the determination of limits on the half-life for the two neutrino mode $T_{1/2}^{(2\nu)}(0^+ \rightarrow 2_1^+) > 1.1 \cdot 10^{21}$ y (at 90% C.L.) and for the neutrinoless mode $T_{1/2}^{(0\nu)}(0^+ \rightarrow 2_1^+) > 1.6 \cdot 10^{23}$ y (at 90% C.L.).

Key words: double beta decay, neutrino, ^{100}Mo , excited state

PACS: 23.40.-s; 14.60.Pq

1 Introduction

The main interest in double beta decay is connected with the neutrinoless mode ($0\nu\beta\beta$) as a probe for physics beyond the Standard Model of electroweak interactions. Its existence is connected with fundamental aspects of particle physics, for example, non-conservation of the lepton number, the existence and nature of neutrino mass, the existence of right-handed currents in the electroweak interaction, the existence of a massless Goldstone boson (the Majoron) and the existence of supersymmetry [1,2,3]).

Interest in neutrinoless double beta decay has seen a significant rebirth in recent years after the evidence for neutrino oscillations was obtained from the results of atmospheric [4] and solar [5,6,7,8,9] neutrino experiments (see, for

* Corresponding author.

Email address: Roger.Arnold@IReS.in2p3.fr (R. Arnold).

example, the discussions in [10,11,12]). This observation of oscillations was recently confirmed by the KamLAND experiment with reactor antineutrinos [13] and by the new SNO result [14]. These results are impressive proof that neutrinos have a non-zero mass. However, the experiments studying neutrino oscillations are not sensitive to the nature of the neutrino mass (Dirac or Majorana?) and provide no information on the absolute scale of the neutrino masses, since such experiments are sensitive only to neutrino mass-squared difference Δm^2 . The detection and study of $0\nu\beta\beta$ decay is the only practical method to clarify the following characteristics of the neutrino (see discussions in [15,16,17,18]): (i) neutrino nature (is the neutrino a Dirac or a Majorana particle?), (ii) absolute neutrino mass scale (a measurement or a limit on m_1), (iii) the type of neutrino mass hierarchy (normal, inverted, or quasi-degenerate), (iv) CP violation in the lepton sector (measurement of the Majorana CP-phases, which requires high precision neutrino oscillation data and reliable nuclear matrix elements).

In connection with the $0\nu\beta\beta$ decay, the detection of double beta decay with emission of two neutrinos ($2\nu\beta\beta$), which is an allowed process of second order in the Standard Model, provides the possibility for experimental determination of the nuclear matrix elements (NME) involved in the double beta decay processes. This leads to the development of theoretical schemes for nuclear matrix-element calculations both in connection with the $2\nu\beta\beta$ decays as well as the $0\nu\beta\beta$ decays (see, for example, [19]). At present, $2\nu\beta\beta$ to the ground state of the final daughter nucleus has been measured for ten nuclei: ^{48}Ca , ^{76}Ge , ^{82}Se , ^{96}Zr , ^{100}Mo , ^{116}Cd , ^{128}Te , ^{130}Te , ^{150}Nd and ^{238}U (a review of results is given, for example, in Refs. [20,21]).

The $\beta\beta$ decay can proceed through transitions to the ground state as well as to various excited states of the daughter nucleus. Studies of the latter transitions allow supplementary information about $\beta\beta$ decay to be obtained. Because of smaller transition energies, the probabilities for $\beta\beta$ -decay transitions to excited states are substantially suppressed in comparison with transitions to the ground state. The first exclusive studies of $\beta\beta-\gamma$ coincidence experiments have been done on ^{100}Mo about 15 year ago [22]. But as it was shown in Ref. [23], by using low-background facilities utilising High Purity Germanium (HPGe) detectors, the $2\nu\beta\beta$ decay to the 0_1^+ level in the daughter nucleus may be detected for such nuclei as ^{100}Mo , ^{96}Zr and ^{150}Nd . In this case the energies involved in the $\beta\beta$ transitions are large enough (1903, 2202 and 2627 keV, respectively), and the expected half-lives are of the order of $10^{20} - 10^{21}$ y. The required sensitivity was only reached for ^{100}Mo (the transition was detected in three independent experiments [24,25,26]) and ^{150}Nd [28]. Recently additional isotopes, ^{82}Se , ^{130}Te , ^{116}Cd and ^{76}Ge , have also become of interest to studies of the $2\nu\beta\beta$ decay to the 0_1^+ level (see review in Refs. [21,29]).

Theoretical estimates of the $2\nu\beta\beta$ decay to a 2^+ excited state have shown that

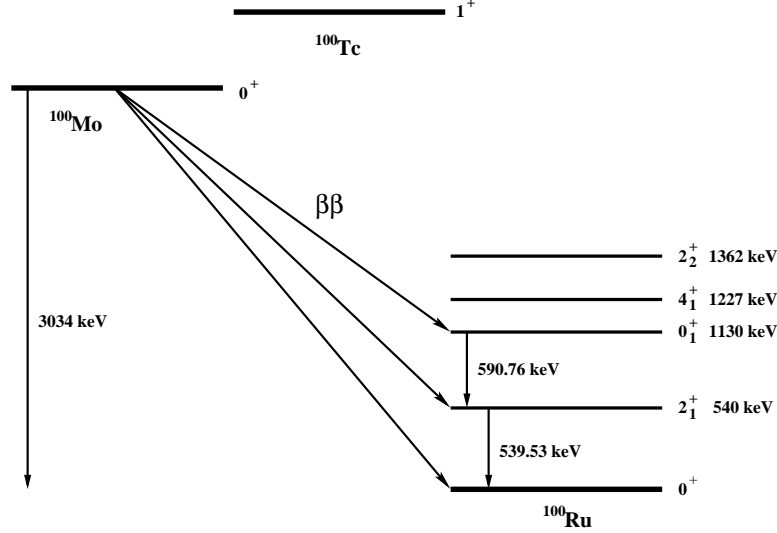


Fig. 1. A double beta decay scheme of ^{100}Mo showing the decay to the ground and excited states of ^{100}Ru . The latter transitions are followed by de-excitation γ -rays.

for a few nuclei (^{82}Se , ^{96}Zr , ^{100}Mo , and ^{130}Te) the half-lives can be $\sim 10^{22} - 10^{23}$ y [30,31]. This would mean that the detection of such decays becomes possible using the present and new installations in the future.

It is very important to note that in the framework of QRPA models the behaviour of NME(2ν) parameter g_{pp} is completely different for transitions to the ground and excited (2^+ and 0^+) states [30,32]. This is why the decay to excited states may probe different aspects of the calculation method than the decay to the ground states. The $0\nu\beta\beta$ transition to excited states of daughter nuclei, which provides a clear-cut signature of such decays, is worthy of special note here: in addition to two electrons with fixed total energy, there appears one ($0^+ - 2^+$ transition) or two ($0^+ - 0^+$ transition) photons, their energies being strictly fixed as well. In a hypothetical experiment detecting all decay products with a high efficiency and a high energy resolution, the background could be reduced nearly to zero. Possibly this idea will be used in future experiments featuring a large mass of the substance under study (as mentioned in Refs. [21,29,33]). In Ref. [34] it was mentioned that detection of this transition will give us the additional possibility to distinguish the $0\nu\beta\beta$ mechanisms (the light and heavy Majorana neutrino exchange mechanisms, the trilinear R-parity breaking mechanisms etc.). So the search for $\beta\beta$ transitions to the excited states has its own special interest.

The ^{100}Mo decay scheme is shown in Fig. 1. The $\beta\beta$ decay to the 0_1^+ excited state of ^{100}Ru is accompanied by the simultaneous emission of two electrons and two γ -rays of the energies of 540 keV and 590 keV. The emission of two electrons and of one γ -ray of energy 540 keV is the signature of the double beta decay to the 2_1^+ excited state.

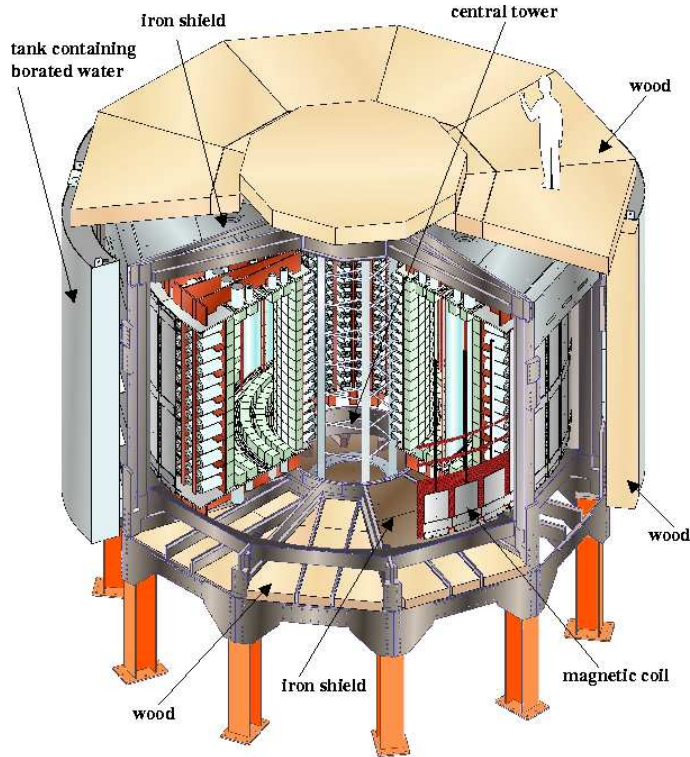


Fig. 2. A schematic view of the NEMO 3 detector.

2 NEMO 3 experiment

NEMO 3 is a currently running experiment searching for neutrinoless double beta decay. The philosophy behind the NEMO 3 detector is the direct detection of the two electrons from $\beta\beta$ decay by a tracking device and a calorimeter [35]. A schematic view of the NEMO 3 detector is shown in Fig. 2. The NEMO 3 detector has three main components, a foil consisting of different sources of double beta decay isotopes and copper, a tracker made of Geiger wire cells and a calorimeter made of scintillator blocks with PMT readout, surrounded by a solenoidal coil. The detector has the ability to discriminate between events of different types by positive identification of charged tracks and photons. The estimated sensitivity of this detector for $0\nu\beta\beta$ decay, a function of both the detector design and the isotope type, is of the order of 10^{25} y, which corresponds to an effective neutrino mass $\langle m_\nu \rangle$ at the level of $0.1 - 0.3$ eV.

2.1 General description

The NEMO 3 detector is cylindrical in design and is composed of twenty equal sectors. The external dimensions of the detector with shields are about 6 m in diameter and 4 m in height. NEMO 3 is based on the techniques tested on

previous incarnations of the experiment NEMO 1 [36], and NEMO 2 [37]:

The wire chamber is made of 6180 open octagonal drift cells which operate in Geiger mode (Geiger cells). A gas mixture of $\sim 95\%$ helium, 4% ethyl-alcohol, 1% argon and 0.15% water at 10 mbar above atmospheric pressure is used as the filling gas of the wire chamber. Each drift cell provides a three-dimensional measurement of the charged particle tracks by recording the drift time and the two plasma propagation times. The transverse position is determined from the drift time, while the longitudinal position is deduced from the difference between the plasma propagation times at both ends of the cathode wires. The average vertex position resolution for the two-electron events is $\sigma_t = 0.5$ cm in the transverse plane of the detector and $\sigma_l = 0.8$ cm in the longitudinal plane. The Geiger counters information is treated by the track reconstruction program based on the cellular automaton algorithm, described in [38].

The calorimeter, which surrounds the wire chamber, is composed of 1940 plastic scintillator blocks coupled by light-guides to very low-radioactivity photomultiplier tubes (PMTs) developed by Hamamatsu. The energy resolution $FWHM/E$ of the calorimeter ranges from 14.1 to 17.6% for 1 MeV electrons, while the time resolution is of 250 ps at 1 MeV.

The apparatus accommodates almost 10 kg of different double beta decay isotopes, comprising ^{100}Mo (6914 g), ^{82}Se (932 g), ^{116}Cd (405 g), ^{130}Te (454 g), ^{150}Nd (34 g), ^{96}Zr (9 g), and ^{48}Ca (7 g). Most of these isotopes are highly enriched, between 95 – 99%, and are produced in the form of thin metallic or composite foils with a surface density of 30 – 60 mg/cm². Three sectors are also used for external background measurement and are equipped respectively with pure Cu (one sector, 621 g) and natural Te (1.7 sectors, 614 g of $^{nat}\text{TeO}_2$). Some of the sources, including ^{100}Mo , have been purified in order to reduce their content of ^{208}Tl (from ^{232}Th and ^{228}Th , and from ^{228}Ra with half-life of 5.75 y) and ^{214}Bi (from ^{226}Ra with half-life of 1600 y) either by a chemical procedure [39], or by a physical procedure [35]. The foils are placed inside the wire chamber in the central vertical plane of each sector. The majority of the detector, 12 sectors, is mounted with 6.9 kg of ^{100}Mo .

The detector is surrounded by a solenoidal coil which generates a vertical magnetic field of 25 Gauss inside the wire chamber. This magnetic field allows electron-positron separation by measuring the curvature of tracks. The ambiguity of the e^+/e^- recognition based on the curvature reconstruction is 3% at 1 MeV.

The whole detector is covered by two types of shielding against external γ -rays and neutrons. The inner shield is made of 20 cm thick low radioactivity iron and stops γ -rays and slow neutrons. The outer shield, comprised of tanks filled with borated water on the vertical walls and wood on the top and bottom,

was designed in order to thermalise and capture neutrons.

The experiment is located in the Fréjus Underground Laboratory, the LSM¹, at the depth of 4800 m water equivalent where the remaining cosmic ray flux is only 4.2 muons per m² per day [40]. In May 2002 the detector took its first data which were used for the study of the detector's performance. Since February 2003, after the final tuning of the experimental set-up, NEMO 3 has routinely been taking data devoted to double beta decay studies. The calibration with radioactive sources is carried out every 6 weeks. The stability of the calorimeter is checked daily with a laser based calibration system [35].

The advantage of the NEMO 3 detector rests in its capability to identify the two electrons from $\beta\beta$ decay and the de-excitation photons from the excited state of the daughter nucleus. The NEMO 3 calorimeter also measures the detection time of the particles. The use of appropriate time-of-flight (TOF) cuts, in addition to energy cuts, allows an efficient reduction of all backgrounds.

2.2 Background

According to its origin, the background events in NEMO 3 can be divided into two categories. The first category is called *internal background* and has its origin inside the source *foils*. This background is mainly due to the presence of radioactive impurities in the foils. Particularly dangerous are β^- -emitters with high Q_β values like ²⁰⁸Tl ($Q_\beta = 4.99$ MeV) and ²¹⁴Bi ($Q_\beta = 3.27$ MeV). These isotopes can produce $\beta\beta$ -like events through three mechanisms: (i) a β -decay accompanied by an electron conversion process, (ii) the Möller scattering of a β -decay electron, and (iii) a β -decay emission to an excited state followed by the Compton scattering of the de-excitation photon.

Great care was taken in the production and subsequent purification of the enriched materials, as well as during the source foil fabrication itself and its installation into the detector to keep any background contamination to the minimum. The source foils were required to satisfy strict radioactivity limits [35].

In addition to the radioactive impurities, the $2\nu\beta\beta$ (g.s. \rightarrow g.s.) decay is also a source of internal background for the $2\nu\beta\beta$ decay to excited states signal because of bremsstrahlung radiation from the electrons. The tail of the E_{ee} distribution from $2\nu\beta\beta$ overlaps the window of interest, to some extent, for the $0\nu\beta\beta$ decay search. Its contribution depends on the $2\nu\beta\beta$ decay half-life and the energy resolution of the detector.

¹ Laboratoire Souterrain de Modane; <http://www-lsm.in2p3.fr>

The second category of background in the NEMO 3 experiment is called *external background* and is caused by electrons or photons generated everywhere else except within the foils. One component of this background is due to radioactive isotopes present in the detector construction materials. This contribution was minimised by a strict selection of low radioactivity materials during the NEMO 3 construction [35,41]. Another component comes from the laboratory walls and from radon present in the laboratory air. Background from cosmic rays is negligible thanks to the placement of the detector in the underground site. Neutron background is also negligible due to the two types of shields against neutrons and γ -rays (from neutron capture) and because of use of the magnetic field, which during data processing allows the elimination of e^+e^- pairs coming from the interaction of high energy photons with the source foils.

The most bothersome external background contribution comes from radon. Radon is a highly diffusive radioactive gas and is outgassed into the air from the rock walls of the LSM laboratory. It can enter the detector either through tiny gaps between the sectors, or through gas piping joints. The average radon activity in air of the LSM laboratory is around 10 – 20 Bq/m³, while the measured value of average volume activity of radon inside the NEMO 3 input gas from February 2003 to September 2004 was about 25 – 30 mBq/m³. Radon disintegrates to ²¹⁴Pb via two α -decays. The latter, after a subsequent β^- -decay, generates ²¹⁴Bi. The decay of ²¹⁴Bi to ²¹⁴Po is generally accompanied by one electron and several photons, it has a recognisable signature consistent with a real $\beta\beta$ event and can only be partially rejected by the TOF cuts. ²¹⁴Po is an α -emitter ($T_{1/2} = 163 \mu\text{s}$) and decays to ²¹⁰Pb. NEMO 3 records events with a delay time up to 700 μs in order to tag the α -particles from the ²¹⁴Po.

3 Analysis and results

In this work we use the data taken from March 17, 2003 up to September 23, 2004. This time corresponds to the stable period of the operation of the NEMO 3 detector before the installation of an anti-radon factory in order to reduce radon background. The efficient data collection time is 8024 hours (0.92 y) and the total number of triggers was $2.2 \cdot 10^8$.

3.1 Particle identification in NEMO 3

The NEMO 3 detector is capable of identifying electrons, positrons, photons, and α -particles by unambiguous topological signatures. We define them in the following way:

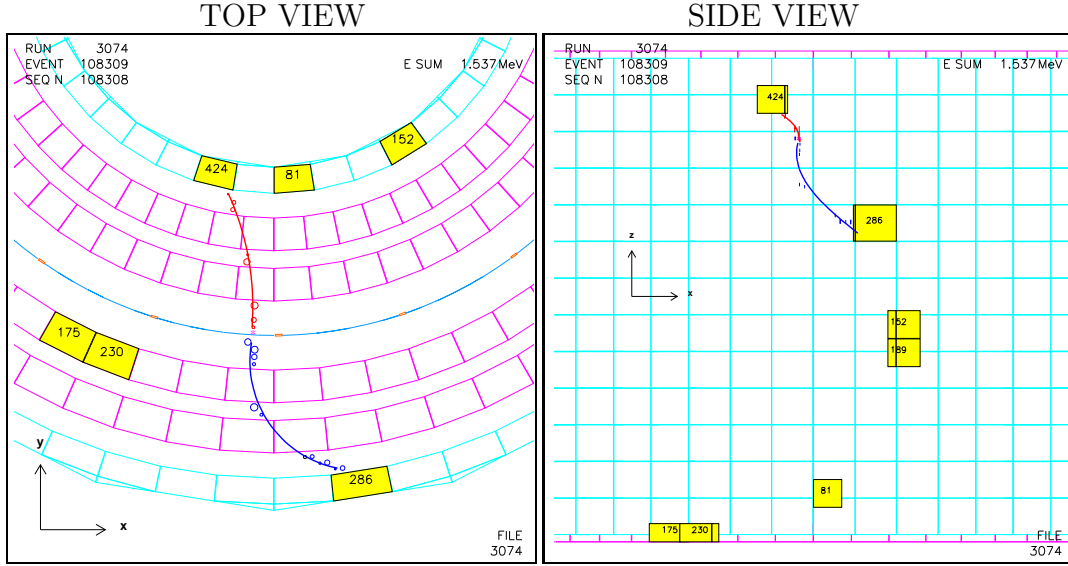


Fig. 3. Top (left) and side (right) views of a reconstructed event candidate selected from data. Two electrons of 424 and 286 keV energy hit fired isolated scintillators. They have a common origin in the source foil. The remaining fired scintillators compose three γ -clusters of 405 (175+230) keV, 341 (152+189) keV and 81 keV. The two clusters of highest energy are due to γ -rays emitted in coincidence with the electrons. The third cluster is most probably due to the rescattering of one of these γ -rays. In this event the total deposited energy is 1537 keV.

- An electron coming from the source foil is recognised as a track going anticlockwise ("negative" track curvature), found by the track reconstruction program and pointing to a fired scintillator. The scintillator has to be isolated from all other fired scintillators.
- A positron is defined like an electron but with the opposite ("positive") track curvature.
- A photon is defined as a group of one or more fired scintillators, in the same region of the detector, unassociated with any track. It is required that all the scintillators in the group have to be fired close together in time in order to exclude a random coincidence of hits of different origin.
- An α -particle is defined as a group of delayed Geiger cell hits, which are in time within $1.5 \mu\text{s}$ and close to each other in space. It is required that an α -particle has to be close to the event vertex or to the electron (positron) track.

An example of a typical real event, selected for the study of the double beta decay of ^{100}Mo to the excited 0_1^+ state, is shown in Fig. 3.

3.2 Background estimation methods

Two different methods of background estimation are used here to evaluate the decay half-life: the first one is based on Monte-Carlo (MC) simulations

(Method 1) [42], while the second one is based on event analysis in selected non-Molybdenum foils (Method 2).

The Method 1 requires the knowledge of activities of all the background sources. These activities have been measured by the HPGe detectors in the LSM laboratory and by radon detectors [35]. A special data analysis allowed the verification of these radioactive contamination levels and further, to determine them with higher precision.

The presence of non-Molybdenum foils in the NEMO 3 set-up allows them to be used for independent background estimation and to provide a cross check (Method 2) to the result obtained with the Method 1. The foils made of Copper, natural and enriched Tellurium, Selenium and Cadmium are used to this end. It is supposed that the contribution from double beta decay to the excited states of other sources such as Tellurium, Selenium and Cadmium can be neglected due to the greater predicted half-lives than for Molybdenum [30,43]. Consequently, the events selected in the non-Molybdenum foils are expected to be composed only of the sum of the contributions of the internal foil contaminations specific for each source and of the common external background, where the main background component is due to radon in the tracking wire chamber. Knowing the internal contamination values for each source foil [35], one can evaluate the contribution corresponding to the radon background. The number of events due to the internal foil contamination evaluated by MC calculation is found to be negligibly small compared to the number due to the radon background. The number of events from the radon background in non-Molybdenum foils is used to evaluate the radon background in Molybdenum by scaling in proportion to their foil surfaces. The correction due to the variation of the event registration efficiency for different detector parts has been also applied. The recalculation coefficient is determined to be equal to 1.7.

For Method 2 it is not necessary to know the absolute level of the main background from MC simulation. This is an advantage of the method. However its accuracy is limited by low statistics of observed events in non-Molybdenum foils.

3.3 Event selection

In this section we described just the common selection criteria for the four channels of analysis. Other criteria specific for the different channels are given in the section devoted to the each analysis (see Secs. 3.4, 3.5, 3.6 and 3.7).

Only events containing two electrons coming from the source foils and each depositing energy greater than 200 keV in the scintillators are selected. It is

required that each track be associated with a unique scintillator which must have a gain greater than $0.17 \text{ (keV/ADC channel)}^{-1}$. Only the tracks starting from the first two Geiger cell layers are kept. The track intersection with the source foil is called a track vertex and then the event vertex, i.e. the presumed double beta decay origin in the source foil, is the average position of the track vertices. Each event has to have its vertex on the source foil. The distance between the track vertex and the event vertex is set to be within 2 cm in the drift plane and within 4 cm in the vertical direction. In order to prevent the wrong determination of the charge of shorter tracks, the events with a track associated with the scintillators on the top or bottom endcaps of the detector close to the source foils are rejected.

To determine whether the origin of the electrons in the event is the source foil (“internal”) or outside the foil (“external”), the time of flight of both particles is used to calculate the corresponding probability of each hypothesis P_{int} and P_{ext} [35]. The event is accepted as a double beta decay candidate if $P_{\text{int}} > 0.01$ and $P_{\text{ext}} < 0.001$.

According to the decay scheme the number of γ -rays simultaneously emitted from the event vertex (“internal γ -ray”) must be exactly two for the decay to the 0_1^+ state and exactly one for the decay to the 2_1^+ state. The estimation of the probability that the γ -ray was emitted together with each electron from the source foil (*internal hypothesis*) or crossing the tracking chamber (*external hypothesis*) was based on the time-of-flight information. Only events with probabilities for electron- γ pairs $P_{\text{int}} > 0.01$ and $P_{\text{ext}} < 0.01$ are selected.

In order to suppress the background contribution due to the radon in the tracking chamber, events with α -particles must be excluded. The tagging of α -particles allows the reduction of the radon background contribution by $\approx 40\%$.

3.4 $2\nu\beta\beta$ decay of ^{100}Mo to the 0_1^+ excited state of ^{100}Ru

Since in the double beta decay to the 0_1^+ excited state there are two electrons and two γ -rays, it is required that the number of γ -clusters must be greater or equal to two. This selection criterion is motivated by the fact that a γ -ray emitted from the source foil can be scattered off a scintillator depositing in it some energy and then hit another scintillator. This requirement allows us to increase the efficiency of the signal selection. The corresponding information about the proportion of events with one, two or more γ -clusters for the data and MC is given in Table 1.

According to the decay scheme, the energy of each emitted γ -ray can not be greater than 590 keV. In order to obtain the biggest signal-to-background ratio (S/B), the upper limit on γ -cluster energy is set to 550 keV and, at the same

Table 1

The relative fraction of events with different numbers of γ -clusters for the data and MC simulation of the signal and the main background, radon, in the tracking chamber inside NEMO 3.

Number of γ -clusters per event	Experiment	MC simulation of $2\nu\beta\beta$ ($0^+ \rightarrow 0_1^+$) of ^{100}Mo	MC simulation, radon background
1	24.6%	15.6%	24.1%
2	56.7%	56.2%	55.2%
3	14.4%	21.5%	16.9%
>3	4.3%	6.7 %	4.4%

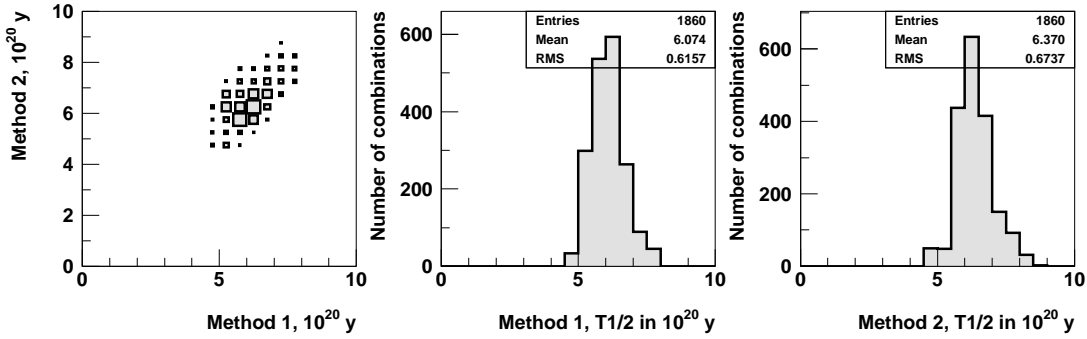


Fig. 4. Half-lives ($T_{1/2}$) of the double beta decay of ^{100}Mo to the 0_1^+ excited state of ^{100}Ru , obtained by the two analysis methods for 1860 combinations of kinematic cuts.

time, the energy of a cluster corresponding to the “internal γ -ray” cluster has to be greater than 100 keV. However, if the energy of an extra fired scintillator which is not an “internal photon” is more than 150 keV, the event is rejected. This requirement allows us to suppress events originating from an external γ -ray that deposits a part of its energy in one scintillator and then interacts with the source foil imitating the signal process.

160 events remained in the data after this event selection. The total number of background events defined by Method 1 and Method 2 is found to be 71.4 and 68.4 events, respectively. According to both background estimation methods the background is mostly due to the radon in the tracking volume of NEMO 3. To suppress this radon component in the background, events with the cosine of the angle between the two photons less than 0.8 are selected (Fig. 5(e)). A total of 1860 combinations of cuts on the following kinematic parameters has been carried out: the upper limit for the energy sum of the two electrons (E_{ee}^{max}): from 1000 keV to 1900 keV in steps of 100 keV; the upper limit on the energy of each electron (E_e^{max}): from 600 keV to 1000 keV in steps of

Table 2

The results for the $2\nu\beta\beta$ decay to the 0_1^+ excited state: the signal registration efficiency (ε), signal-to-background ratio (S/B), total number of selected events (S+B) and statistical significance of the signal ($N\sigma = S/\sqrt{S+B}$) for the two analysis methods. Results for both methods are given for the same kinematic cuts on the variables: E_{ee}^{\max} , E_e^{\max} , $E_{\gamma\gamma}^{\min}$, E_γ^{\min} .

method	Kinematic cuts in keV				$\varepsilon \cdot 10^{-4}$	S/B	S+B	$N\sigma$
	E_{ee}^{\max}	E_e^{\max}	$E_{\gamma\gamma}^{\min}$	E_γ^{\min}				
Method 1	1200	700	500	125	8.1 ± 1.0	3.0	50	5.3
Method 2	1200	700	500	125	8.1 ± 1.0	3.2	50	5.4

50 keV; the lower limit on the energy sum for two “internal γ -rays” ($E_{\gamma\gamma}^{\min}$): from 300 keV to 800 keV in steps of 100 keV; the lower limit on the energy of each “internal γ -ray” (E_γ^{\min}): from 125 keV to 250 keV in steps of 25 keV. For each combination of cuts the two methods of background estimation are used. For each, the results of the calculations of the half-lives for both analysis methods as well as the correlation between them are shown in Fig. 4. The two methods give almost the same average value of the half-life around $6 \cdot 10^{20}$ y and are in a very good agreement (see Fig. 4).

Finally, after the cut optimisation we have chosen the kinematic cuts providing the maximal value of the product $S/B \times \varepsilon$ using Method 1, where ε is the signal registration efficiency. The optimal set of cuts for this criterion is given in Table 2.

The distributions of the decay characteristics of selected events for Method 1 after applying optimal kinematic cuts are shown in Fig. 5(I) and the corresponding background component contributions evaluated by this method are shown in Table 3. In Fig. 5(II) the same spectra obtained using Method 2 are present. The numbers of signal and background events after the cuts obtained for Method 1 are: $37.5 \pm 7.1(\text{stat.}) \pm 5.2(\text{syst.})$ and $12.5 \pm 2.9(\text{syst.})$. For Method 2 the numbers are $38.2 \pm 8.4(\text{stat.}) \pm 4.7(\text{syst.})$ and $11.8 \pm 4.5(\text{stat.}) \pm 0.4(\text{syst.})$.

The estimation of the systematic uncertainty has been made taking into account the following contributions:

- The two electron detection inefficiency due to the inaccuracy of the GEANT simulation and inaccuracy of the tracking program is estimated to be less than 5%. It is determined by reproducing the activity of the calibrated source placed inside the NEMO 3 detector.
- The efficiency calculation error due to the inaccuracy of the GEANT simulation for γ -rays is found by comparing the MC simulation and data from the calibration source. For the two γ -channel it is estimated to be around

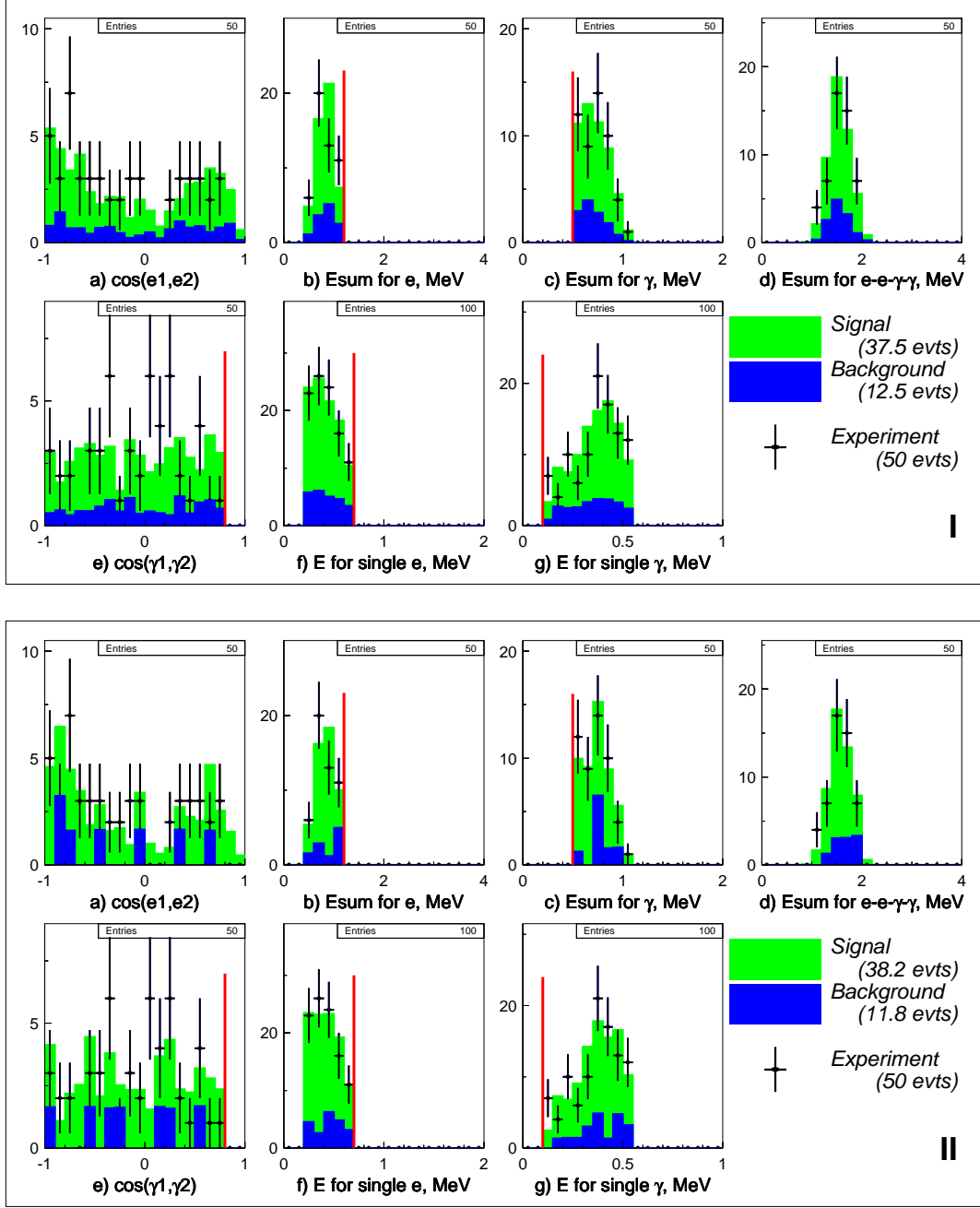


Fig. 5. The main characteristics of selected events for the study of $2\nu\beta\beta$ decay of ^{100}Mo to the 0_1^+ excited state of ^{100}Ru after the final kinematic cut application for Method 1 (I) and for Method 2 (II): (a) the distribution of the cosine of the angle between the two electrons, (b) the energy sum of the two electrons, (c) the energy sum of the two γ -rays, (d) the total energy sum, (e) the distribution of the cosine of the angle between the two γ -rays, (f) the energy of each electron, (g) the energy of each γ -ray. The experimental points are shown in black, the MC simulation of the background in blue, the simulation of the signal process in green. The fixed positions of the kinematic cuts for the best result are presented with red lines ($E_{ee}^{\max} = 1.2$ MeV, $E_e^{\max} = 0.7$ MeV, $E_{\gamma\gamma}^{\min} = 0.5$ MeV, $E_{\gamma}^{\min} = 0.125$ MeV).

Table 3

The calculated number of events in the observed spectrum for ^{100}Mo foils from each background component. Only the components leading to a number of expected events greater than 0.1 are given here.

Background component	$2\nu\beta\beta$ (to g.s.)	internal ^{214}Bi	internal ^{208}Tl	^{214}Bi (radon inside tracking chamber)	^{214}Bi (radon outside tracking chamber)
Number of events	0.5	0.2	0.3	11.2	0.3

10%.

- The effect of the uncertainty in the energy calibration coefficients causes a 2% contribution to the systematic error in the half-life. It has been estimated by the energy scale variation for the experimental data.
- The effect of the single electron energy threshold for the two electron signal is estimated as 3%.
- The effect of the uncertainty of the detector efficiency is evaluated from the comparison of results of the $2\nu\beta\beta$ decay to the ground state separately for metallic and composite foils of ^{100}Mo . It is estimated to be around 4%.
- The uncertainty of the radon level measurement is 20% which gives a 6% error in the half-life. This uncertainty is inherent only in analysis Method 1. All other background uncertainties do not introduce any significant error into the evaluation of result.

The total systematic error on the result of analysis Method 1 is 13.8%, and of the Method 2 is 12.4%. It is comparable with the spread of the half-lives for the 1860 kinematic cut combinations presented in Fig. 4.

The final results of the half-life measurements for the two neutrino double beta decay of ^{100}Mo to the 0_1^+ excited state of ^{100}Ru for both methods are the following:

$$T_{1/2}^{(2\nu)}(0^+ \rightarrow 0_1^+) = 5.7_{-0.9}^{+1.3}(\text{stat.}) \pm 0.8(\text{syst.}) \cdot 10^{20} \text{ y (Method 1);}$$

$$T_{1/2}^{(2\nu)}(0^+ \rightarrow 0_1^+) = 5.6_{-1.0}^{+1.5}(\text{stat.}) \pm 0.7(\text{syst.}) \cdot 10^{20} \text{ y (Method 2).}$$

3.5 Search for the $0\nu\beta\beta$ decay to the 0_1^+ excited state of ^{100}Ru

For the study of the neutrinoless double beta decay of ^{100}Mo to the 0_1^+ excited state of ^{100}Ru , in addition to the selection criteria described in Sec. 3.3, the energy of each electron is required to be less than 1600 keV and the energy of each photon (E_γ) to be greater than 125 keV and less than 600 keV according to the particle energy distributions for the 0ν mode.

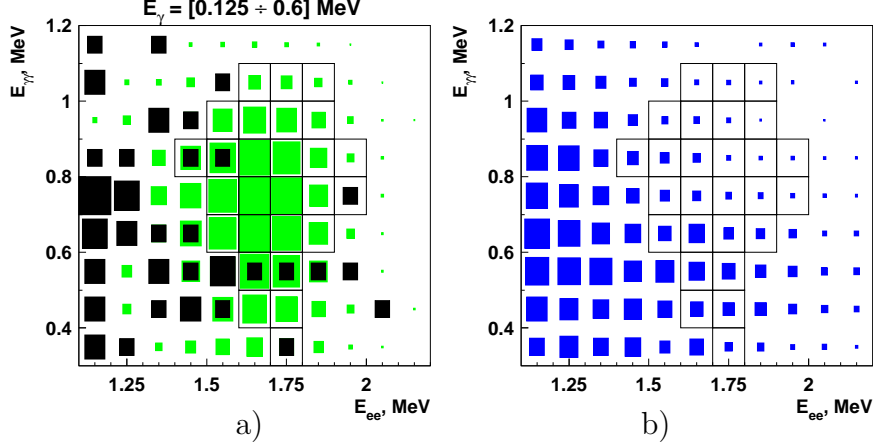


Fig. 6. Scatter plot of the sum of the γ -rays energy versus the energy sum of the electrons a) for the data (in black) and b) for the MC background (in blue). The simulated $0\nu\beta\beta$ to the 0_1^+ excited state signal ((a), in green) is also shown with an arbitrary scale. The bins with $\varepsilon_S/\varepsilon_B > \langle\varepsilon_S/\varepsilon_B\rangle$ are shown with a black frame.

The two-dimensional distribution of the energy sum of the two γ -rays ($E_{\gamma\gamma}$) and the energy sum of the two electrons (E_{ee}) is shown in Fig. 6. The expected signal (ε_S) and the background (ε_B) efficiencies can be found for each bin of this distribution from the MC simulation. The signal-to-background ratio ($\varepsilon_S/\varepsilon_B$) may be calculated for each bin, and their average value $\langle\varepsilon_S/\varepsilon_B\rangle$ among all bins is found. It is reasonable to consider only the bins with a significant ε_S . If $\varepsilon_S/\varepsilon_B > \langle\varepsilon_S/\varepsilon_B\rangle$ is required, the region searched is composed of 27 bins (see the Fig. 6). 6 experimental events are observed and 6.6 MC background events are expected. Comparing experimental data with the MC background there is no evidence for the 0ν signal.

To set the limit we apply a method based on the confidence level computation with small statistics (CLs method) [44] treating each bin of the distribution as independent search channel. The uncertainty in the number of background events has been set at 20% (mostly due to the radon level uncertainty), for the signal efficiency error we use 5%. Using the MCLIMIT program [45] the number of signal events excluded at 90% confidence level is calculated to be 3.9. Taking into account the signal efficiency of 1.3% one may evaluate the limit on the 0ν decay half-life:

$$T_{1/2}^{(0\nu)}(0^+ \rightarrow 0_1^+) > 8.9 \cdot 10^{22} \text{y (at 90\% C.L.)}$$

3.6 Search for the $2\nu\beta\beta$ decay of ^{100}Mo to the 2_1^+ excited state of ^{100}Ru

This decay produces the emission of two electrons and one photon of 540 keV (Fig. 1). To study this decay channel we perform the same data selection as

for the decay to the 0_1^+ excited state but with the modified criterion that the number of fired scintillators in event is required to be greater than or equal to 3. The energy sum of all γ -clusters must be less than 550 keV. In order to select events in the energy region specific for this decay channel, we used the following kinematic cuts for event selection: the total detected energy must be greater than 1000 keV; the energy of the “internal γ -ray” must be greater than 250 keV; the cosine angle between an electron and the γ -ray must be less than 0.8. The latter cut is used in order to suppress the possible background from the double beta decay to the ground state accompanied by a γ -ray tangent to one of electrons emitted by the Bremsstrahlung process in the source foil.

531 events result from this selection, 465 of them can be attributed to the background according to analysis Method 1. The main background contributions according to the MC simulations come from the radon in the tracking chamber (38% of total background), $2\nu\beta\beta$ decay to the 0_1^+ excited state (15%), $2\nu\beta\beta$ decay to the ground state (15%), radon outside the tracking chamber (12%) and internal radioactive contamination of PMTs in ^{232}Th (12%) and ^{226}Ra (12%). The error on the signal (σ) is 43.2 and includes also the systematic uncertainty of the background calculation. The statistical significance of the disagreement between MC and data is 1.5σ . Using the signal efficiency defined by the MC simulation (0.45%) the half-life limit of the $2\nu\beta\beta$ decay of ^{100}Mo to the 2_1^+ excited state of ^{100}Ru is calculated to be:

$$T_{1/2}^{(2\nu)}(0^+ \rightarrow 2_1^+) > 1.1 \cdot 10^{21} \text{ y (at 90\% C.L.)}$$

3.7 Search for the $0\nu\beta\beta$ decay of ^{100}Mo to the 2_1^+ excited state of ^{100}Ru

A similar analysis to that described in Sec. 3.5 has been performed to search for the neutrinoless double beta decay of ^{100}Mo to the 2_1^+ excited state. After the preliminary analysis the events with the typical topology were selected and the two-dimensional distribution of the energy sum of the electrons E_{ee} and the energy of the γ -rays E_γ was analysed.

Using the same approach as for the $2\beta0\nu$ ($0^+ \rightarrow 0_1^+$) (see sect. 3.5) there are 31 bins of the distribution with $\varepsilon_S/\varepsilon_B$ ratio greater than the average as shown in Fig. 7. The signal efficiency is found to be 2.9%², 6 events are observed and 5.7 background events are expected. In the limit calculations the background uncertainty (20% mostly due to the radon level uncertainty) and the error on the signal efficiency (5%) have been taken into account. 4.9 signal events are excluded on 90% C.L. and the corresponding limit on the half-life is:

$$T_{1/2}^{(0\nu)}(0^+ \rightarrow 2_1^+) > 1.6 \cdot 10^{23} \text{ y (at 90\% C.L.)}$$

² The N* mechanism of $\beta\beta$ decay [46] has been used for MC simulation.

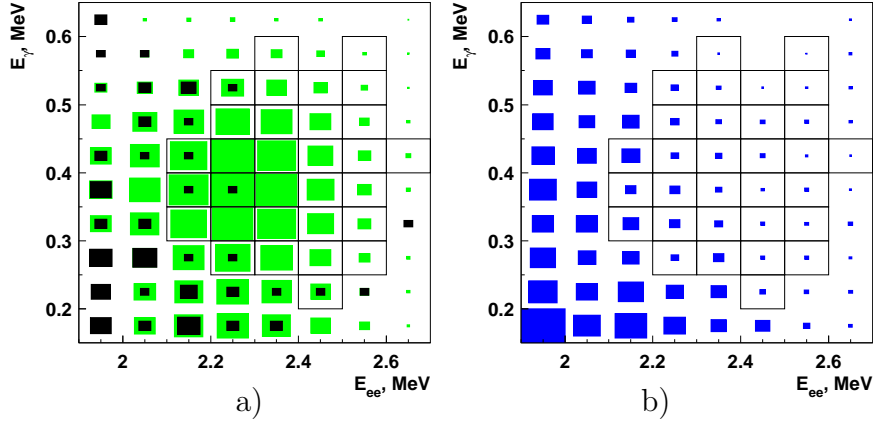


Fig. 7. Scatter plot of the γ -ray energy versus the energy sum of electrons a) for the experimental data (in black) and b) for MC background (in blue). The simulated $0\nu\beta\beta$ to the 2_1^+ excited state signal in arbitrary scale ((a), in green) is also shown. The relevant bins are shown with a black frame.

4 Discussion

The results of this analysis of the $\beta\beta$ -decay of ^{100}Mo to the excited states of ^{100}Ru are presented in Table 4 along with previous experimental results and theoretical estimates for the half-lives.

For the transition to the 0_1^+ excited state of ^{100}Ru the obtained value is in a good agreement with results of previous experiments. It has to be stressed here that in the present experiment with the NEMO 3 detector, all the decay products (two electrons and two γ -rays) were detected for the first time and hence all the useful information about the decay was obtained (total energy spectrum, single electron spectrum, single γ spectrum, and all angular distributions). In previous experiments either individual γ -rays [24,25], or the coincidence between the two emitted γ -rays [26] were detected but no information about electrons was obtained.

One can compare the measured value with the theoretical predictions, which were obtained using QRPA-based models [49,31,55], and the pseudo-SU(3) model [51]. The present accuracy of the theoretical prediction is directly connected to the accuracy of the nuclear matrix elements (NME) calculations and usually is a factor of ~ 4 for the half-life (factor of ~ 2 for the NME). In view of this, it can be seen that there is a reasonable agreement between the experimental and theoretical values of the half-life.

Recently an estimation of the half-life value for the $2\nu\beta\beta$ ($0^+ \rightarrow 0_1^+$) transition of ^{100}Mo was carried out using the so-called single state dominance hypothesis (SSDH) [31,56] and the recent result for electron capture (EC) transition ^{100}Tc

Table 4

Experimental results and theoretical predictions for the half-life of the $\beta\beta$ -decay of ^{100}Mo to the excited states of ^{100}Ru . All limits (except one specifically mentioned) are at 90% C.L. Theoretical predictions for 0ν mode are presented for $\langle m_\nu \rangle = 1 \text{ eV}$ and $\langle \lambda \rangle = 10^{-6}$.

Transition	$T_{1/2}, \text{ y}$ (this work)	$T_{1/2}, \text{ y}$ (previous works)	$T_{1/2}, \text{ y}$ (theor. predictions)
$0\nu\beta\beta;$ $0^+ \rightarrow 2_1^+$	$>1.6 \cdot 10^{23}$	$>1.4 \cdot 10^{22}$ (68% C.L.) [47]	$6.8 \cdot 10^{30} (\langle m_\nu \rangle)$ $2.1 \cdot 10^{27} (\langle \lambda \rangle)$ [48]
$2\nu\beta\beta;$ $0^+ \rightarrow 2_1^+$	$>1.1 \cdot 10^{21}$	$>1.6 \cdot 10^{21}$ [24]	$3.4 \cdot 10^{22}$ [49] $(5.5-24) \cdot 10^{25}$ [51] 10^{22} [50] $2.1 \cdot 10^{21}$ [31]
$0\nu\beta\beta;$ $0^+ \rightarrow 0_1^+$	$>8.9 \cdot 10^{22}$	$>6 \cdot 10^{20}$ [52]	$(7.6-14.6) \cdot 10^{24}$ $(\langle m_\nu \rangle)$ [53] $2.6 \cdot 10^{26} (\langle m_\nu \rangle)$ [54]
$2\nu\beta\beta;$ $0^+ \rightarrow 0_1^+$	$[5.7_{-0.9}^{+1.3}(\text{stat}) \pm 0.8(\text{syst})] \cdot 10^{20}$	$6.1_{-1.1}^{+1.8} \cdot 10^{20}$ [24] $[9.3_{-1.7}^{+2.8}(\text{stat}) \pm 1.4(\text{syst})] \cdot 10^{20}$ [25] $[5.9_{-1.1}^{+1.7}(\text{stat}) \pm 0.6(\text{syst})] \cdot 10^{20}$ [26] $>1.2 \cdot 10^{21}$ [27]	$(0.7 - 1) \cdot 10^{21}$ [55] $2.1 \cdot 10^{21}$ [49] $1.5 \cdot 10^{21}$ [51] $1.5 \cdot 10^{20}$ [31]

$\rightarrow ^{100}\text{Mo}$ [57]: $T_{1/2}^{(2\nu)}(0^+ \rightarrow 0_1^+) = 4.2 \cdot 10^{20} \text{ y}$ [43] (with an accuracy of $\pm 50\%$ because of such accuracy of the EC transition [57]). This value is in agreement with our result and if in the future the accuracy of the EC transition can be improved, then a comparison between experimental and estimated values will provide the possibility to check more precisely the SSDH prediction.

Using the phase-space value $G = 1.64 \cdot 10^{-19} \text{ y}^{-1}$ (for $g_A = 1.254$) and the obtained half-life value, one obtains the nuclear matrix element value (NME) for the $2\nu\beta\beta$ ($0^+ \rightarrow 0_1^+$) transition, $M(0_1^+) = 0.103 \pm 0.011$. One can compare this value with the NME value for the 2ν -transition to the ground state of ^{100}Ru , which was obtained also with the NEMO 3 detector, $M(\text{g.s.}) = 0.126 \pm 0.005$ (here $T_{1/2}^{(2\nu)} = [7.11 \pm 0.02(\text{stat}) \pm 0.6(\text{syst})] \cdot 10^{18}$ [58] and $G = 8.9 \cdot 10^{-18} \text{ y}^{-1}$ [30]). One can see that $M(\text{g.s.})$ is $\sim 20\%$ greater than $M(0_1^+)$. Nevertheless, these values are very close and, taking into account errors and possible uncertainties, their equality can not be excluded. From the viewpoint of the theory it is important to confirm this difference or to rule it out, in particular to ascertain the validity of the SSDH. Future measurements with the NEMO 3 detector where results for both transitions (to the 0^+ ground

and the 0_1^+ excited states) will be improved, will address this further.

The limit obtained for the $2\nu\beta\beta(0^+ \rightarrow 2_1^+)$ decay is comparable with the limit from Ref. [24] but is 1.5 times lower. In this channel a small excess of events is observed, which probably can be explained by a statistical fluctuation. Future measurements are needed to clarify the status of these extra events. The most optimistic theoretical prediction for ^{100}Mo gives $T_{1/2}^{(2\nu)}(0^+ \rightarrow 2_1^+) \approx 2 \cdot 10^{21} - 10^{22}$ y [50,31] for this type of decay which is not very far from the obtained limit. However, the estimation in the framework of the SSDH, which looks more reasonable, gives a higher value, $T_{1/2} = 1.7 \cdot 10^{23}$ y [43].

Concerning the bound on the $0\nu\beta\beta$ decay of ^{100}Mo to 2_1^+ and 0_1^+ excited states of ^{100}Ru the limits obtained in the present work are better than results of previous experiments by a factor of ~ 10 and ~ 100 , respectively. Using the results of theoretical calculations from Refs. [53] and [54] for the $0\nu\beta\beta$ decay of ^{100}Mo to the 0_1^+ state of ^{100}Ru , one obtains a limit on the effective value of the Majorana mass, $\langle m_\nu \rangle < 9.3 - 12.8$ eV and 60 eV, respectively. It means that to reach a sensitivity to $\langle m_\nu \rangle$ at the level of ~ 0.1 eV, the sensitivity to the half-life has to be at the level of $\sim 10^{27}$ y.

The $0\nu\beta\beta(0^+ \rightarrow 2_1^+)$ decay had long been accepted to be possible only because of the contribution of right-handed currents and it is not sensitive to the neutrino mass contribution. However, in Ref. [48] it was demonstrated that the relative sensitivities of $(0^+ \rightarrow 2_1^+)$ decays to the neutrino mass $\langle m_\nu \rangle$ and the right-handed currents $\langle \eta \rangle$ are comparable to those of $0\nu\beta\beta$ decay to the ground state of the daughter nuclei. At the same time, the $(0^+ \rightarrow 2_1^+)$ decay is relatively more sensitive to $\langle \lambda \rangle$. Using the limit of $T_{1/2} > 1.6 \cdot 10^{23}$ y, the value for the NME from Ref. [48] and the phase-space value from Ref. [59], one can obtain the limits $\langle m_\nu \rangle < 6.5 \cdot 10^3$ eV and $\langle \lambda \rangle < 1.2 \cdot 10^{-4}$.

5 Conclusion

The results from the NEMO 3 detector for ~ 1 year of measurement and with a higher level of background from ^{222}Rn than expected, have been obtained. Data taking will be continued for a further ~ 5 years with an improved level of radon background. It means that the sensitivity of the experiment will be improved by a factor of $\sim 5 - 10$. For example, in the case of $2\nu\beta\beta(0^+ \rightarrow 0_1^+)$ decay ~ 200 events will be detected under conditions of a signal-to-background ratio of ~ 10 and an accuracy for the half-life value reduced by $\sim 10\%$. The sensitivity to the $2\nu\beta\beta(0^+ \rightarrow 2_1^+)$ decay will be on the level of $\sim 10^{22}$ y and it could also yield a chance to detect this type of decay (see Table 4). For the 0ν transitions to the 2_1^+ and 0_1^+ excited states the sensitivity will be $\sim 10^{24}$ y.

Acknowledgements

The authors would like to thank the Fréjus Underground Laboratory staff for their technical assistance in running the experiment. A portion of this work has been supported by the Grant Agency of the Czech Republic (grant No. 202/05/P293). Another portion of this work has been supported by a grant from INTAS (No. 03051-3431), by a NATO grant (PST.CLG.980022) and by a RFBR (No. 06-02-16672a). This work has been partially supported by the ILIAS integrating activity (Contract No. RII3-CT-2004-50622) as part of the EU FP6 programme in Astroparticle Physics.

References

- [1] A. Faessler and F. Šimkovic, *Prog. Part. Nucl. Phys.* **46** (2001) 233.
- [2] S.R. Elliot and P. Vogel, *Annu. Rev. Nucl. Part. Sci.* **52** (2002) 115.
- [3] J.D. Vergados, *Phys. Rep.* **361** (2002) 1.
- [4] H. Sobel *et al.*, *Nucl. Phys. B (Proc. Suppl.)* **91** (2001) 127.
- [5] B.T. Cleveland *et al.*, *Astrophys. J.* **496** (1998) 505.
- [6] S. Fukuda *et al.*, *Phys. Rev. Lett.* **86** (2001) 5651; *Phys. Rev. Lett.* **86** (2001) 5656.
- [7] V.N. Gavrin *et al.*, *Nucl. Phys. B (Proc. Suppl.)* **91** (2001) 36.
- [8] M. Altman *et al.*, *Phys. Lett. B* **490** (2000) 16.
- [9] Q.R. Ahmad *et al.*, *Phys. Rev. Lett.* **89** (2002) 011301; *Phys. Rev. Lett.* **89** (2002) 011302.
- [10] P.C. de Holanda and A.Yu. Smirnov, *Phys. Rev. D* **66** (2002) 113005.
- [11] J.N. Bahcall *et al.*, *J. High Energy Phys.* **0207** (2002) 054.
- [12] M. Maltoni *et al.*, *Phys. Rev. D* **67** (2003) 013011.
- [13] K. Eguchi *et al.*, *Phys. Rev. Lett.* **90** (2003) 021802.
- [14] S.N. Ahmed *et al.*, *Phys. Rev. Lett.* **92** (2004) 181301.
- [15] S. Pascoli, S.T. Petcov and W. Rodejohann, *Phys. Lett. B* **558** (2003) 141.
- [16] S. Pascoli and S.T. Petcov, *Phys. Lett. B* **580** (2004) 280.
- [17] S.M. Bilenky, [hep-ph/0403245](#).
- [18] S. Pascoli, S.T. Petcov and T. Schwetz, [hep-ph/0505226](#).

- [19] V.A. Rodin *et al.*, Phys. Rev. **C 68** (2003) 044302; nucl-th/0503063.
- [20] A.S. Barabash, Czech. J. Phys. **52** (2002) 567.
- [21] A.S. Barabash, Phys. At. Nucl. **67** (2004) 438.
- [22] N. Kudomi, *et al.*, Phys. Rev. **46** (1992) R2132.
- [23] A.S. Barabash, JETP Lett. **51** (1990) 207.
- [24] A.S. Barabash *et al.*, Phys. Lett. B **345** (1995) 408.
- [25] A.S. Barabash *et al.*, Phys. At. Nucl. **62** (1999) 2039.
- [26] L. De Braeckeleer *et al.*, Phys. Rev. Lett. **86** (2001) 3510.
- [27] D. Blum *et al.*, Phys. Lett. **B 275** (1992) 506.
- [28] A.S. Barabash, F. Hubert, Ph. Hubert, and V.I. Umatov, JETP Lett. **79** (2004) 10.
- [29] A.S. Barabash, Czech. J. Phys. **50** (2000) 447.
- [30] J. Suhonen and O. Civitarese, Phys. Rep. **300** (1998) 123.
- [31] O. Civitarese, J. Suhonen, Nucl. Phys. **A 653** (1999) 321.
- [32] M. Aunola, J. Suhonen, Nucl. Phys. **A 602** (1996) 133.
- [33] J. Suhonen, Phys. Rev. **62** (2000) 042501.
- [34] F. Šimkovic and A. Faessler, Prog. Part. Nucl. Phys. **48** (2002) 201.
- [35] R. Arnold *et al.* (NEMO Collaboration), Nucl. Instr. and Meth. **A 536** (2005) 79.
- [36] D. Dassié *et al.* (NEMO Collaboration), Nucl. Instr. and Meth. **A 309** (1991) 465.
- [37] R. Arnold *et al.* (NEMO Collaboration), Nucl. Instr. and Meth. **A 354** (1995) 338.
- [38] I. Kisel *et al.* (NEMO Collaboration), Nucl. Instr. and Meth. **A 387** (1997) 433.
- [39] R. Arnold *et al.* (NEMO Collaboration), Nucl. Instr. and Meth. in Phys. Res. **A 474** (2001) 93.
- [40] C. Berger *et al.*, Nucl. Instr. and Meth. in Phys. Res. **A 262** (1987) 463.
- [41] J. Busto *et al.*, Nucl. Instr. and Meth. in Phys. Res. **A 492** (2002) 35.
- [42] L. Vála, Ph.D. Thesis, LAL 03-51 (2003).
- [43] P. Domin *et al.*, Nucl. Phys. **A 753** (2005) 337.
- [44] Th. Junk, Nucl. Instr. and Meth. **A 434** (1999) 435.

- [45] <http://cern.ch/thomasj/searchlimits/ecl.html>
- [46] M. Doi *et al.*, Progr. Theor. Phys. **66** (1981) 1739.
- [47] H. Ejiri *et al.*, Nucl. Phys. **A 611** (1996) 85.
- [48] T. Tomoda, Phys. Lett. **B 474** (2000) 245.
- [49] S. Stoica and I. Mihut, Nucl. Phys. **A 602** (1996) 197.
- [50] J. Schwieger, F. Šimkovic and A. Faessler, Phys. Rev. **C 57** (1998) 1738.
- [51] J.G. Hirsch *et al.*, Phys. Rev. **C 51** (1995) 2252.
- [52] D. Dassié *et al.* (NEMO Collaboration), Phys. Rev **D 51** (1995) 2090.
- [53] F. Šimkovic *et al.*, Phys. Rev. **C 64** (2001) 035501.
- [54] J. Suhonen, Nucl. Phys. **A 700** (2002) 649.
- [55] A. Griffiths and P. Vogel, Phys. Rev. **C 46** (1992) 181.
- [56] J. Abad *et al.*, An. Fis. Ser. **A 80** (1984) 9.
- [57] A. Garcia *et al.*, Phys. Rev. **C 47** (1993) 2910.
- [58] R. Arnold *et al.* (NEMO Collaboration), Phys. Rev. Lett. **95** (2005) 182302.
- [59] T. Tomoda, Rep. Prog. Phys. **54** (1991) 53.